Available online at www.sciencedirect.com
ScienceDirect
Journal of Sound and Vibration 313 (2008) 567–580
JOURNAL OF SOUND AND VIBRATION
www.elsevier.com/locate/jsvi

Identification of complex shear modulus from measured shear strains on a circular disc subjected to a transient torque

S. Mousavi*, L. Hillström, B. Lundberg

The Ångström Laboratory, Uppsala University, Box 534, SE-751 21 Uppsala, Sweden

Received 17 June 2007; received in revised form 7 November 2007; accepted 10 December 2007
Handling Editor: A.V. Metrikine
Available online 29 January 2008

Abstract

A method for identification of complex shear modulus from measured shear strains on a circular disc subjected to a transient torque at its centre has been established. It is based on the evolution of an outgoing shear wave between two radial positions at which the associated shear strains are measured. The two-dimensional shear wave solutions used are exact in the sense of three-dimensional theory. Therefore, in principle, there is no frequency beyond which they are not valid. The method requires a minimum disc size, which is related to the duration of the load. The non-parametric results become inaccurate at frequencies near zero and at certain problematic frequencies where the excitation of the disc is weak or non-existent. These frequencies may be moved outside the frequency range of interest by sufficiently decreasing the duration of the load. If there are problematic frequencies within this range, the results of parametric identification become more accurate than those of non-parametric identification. Parametric results from experimental tests with loads having different amplitudes and durations agree well with each other in accord with the assumed linearity of the tested polypropylene material.

1. Introduction

Polymers and other materials with viscoelastic behaviour are common in engineering applications. In their linear regime, such materials are characterized by two independent complex-valued functions of frequency [1] such as the complex extension modulus and the complex shear modulus. Other complex material functions, such as the bulk modulus and the complex Poisson's ratio, can be expressed in terms of these two functions. Theocaris [2] considered the relative magnitudes of the complex modules, and Pritz [3] examined their frequency dependencies. In engineering applications, frequencies of importance are commonly in the range from hundreds of Hz to tens of kHz, where identification methods based on wave propagation can be used.

Viscoelastic waves associated with extension or torsion of a bar specimen can be represented by three complex-valued functions of frequency, viz., a complex wavenumber and two complex amplitudes representing waves travelling through the bar in opposite directions. The complex wavenumber can be

*Corresponding author. Tel: +46 8555 03997; fax: +46 1847 13122.
E-mail addresses: saed.mousavi@angstrom.uu.se, saed@foi.se, saed00@hotmail.com (S. Mousavi).

0022-460X/$ - see front matter © 2007 Elsevier Ltd. All rights reserved.
doi:10.1016/j.jsv.2007.12.010

Nomenclature

a	inner radius
A	function associated with outgoing wave
b	outer radius
B	function associated with ingoing wave
c	complex wave speed
e	residual, error
$\mathbf{e}$	residual vector
f	frequency, function
G	shear modulus, constitutive parameter
H	Hankel function
$\mathbf{p}$	parameter vector
r	radius
t	time
u, v	displacement

Greek letters

β	complex wavenumber
γ	shear strain
Γ	function representing model
η	viscosity
ξ	argument
ρ	density
τ	shear stress
ϕ	angular coordinate, function
ω	angular frequency

Superscripts

d	dissipative
e	elastic
M	measured

Subscripts

1, 2	identification of measurement
a	at inner radius
n	ingoing
opt	optimum
p	outgoing
T	transverse

expressed in terms of the complex extension or shear modulus, the density and the frequency. Therefore, in general, the complex modules can be estimated on the basis of three or more independent measurements of quantities such as displacements, strains, particle velocities or accelerations [4–12]. The number of measurements required is reduced if the conditions are such that one of the two waves travelling in opposite directions can be discarded or if a well-defined boundary condition can be used [13–19]. In the case of flexural waves, five or more independent measurements are generally required [20].

No published work has been found on the use of viscoelastic axially symmetric shear waves in a disc specimen for identification of the complex shear modulus. If a viscoelastic material is available or used as plates rather than bars, it may be advantageous to use a disc specimen. Even if the materials of a plate and a bar have the same name, differences in material behaviour can be expected due to the different geometries and manufacturing processes. For example, the material properties of a plate may have gradients in the thickness direction while those of a bar with circular cross-section may have gradients in the radial direction. In the case of a disc specimen, two-dimensional shear wave solutions that are exact in the sense of three-dimensional theory can be used. Therefore, in principle, there is no frequency beyond which the theoretical basis for such an identification method is not applicable.

Similarly as above, viscoelastic axially symmetric shear waves in a disc specimen can be represented by a complex wavenumber and two complex amplitudes representing outgoing and ingoing shear waves. The complex wavenumber can be expressed in terms of the complex shear modulus, the density and the frequency. Therefore, in general, the complex shear modulus can be estimated on the basis of, e.g., measurement of shear strains at two radial positions and consideration of the boundary condition at the rim of the disc. If the disc is so large that ingoing reflected shear waves can be discarded, two shear strain measurements suffice. In this case, the disc can be considered infinite and therefore the geometry of the rim of the disc is immaterial.

The aim of this study is to develop a method for identification of complex shear modulus that is based on the evolution of viscoelastic axially symmetric shear waves in a disc specimen. In the following section, the theoretical basis for the method will be developed. In Section 3, the method will be studied through numerical simulation, and in Section 4 it will be implemented experimentally. The results of simulations and experimental tests will be discussed in Section 5, and conclusions will be summarized in Section 6.

2. Theory

2.1. Axially symmetric shear waves in a circular disc

Axially symmetric shear waves in a circular disc with inner radius a, outer radius b and constant thicknesses are considered. The material of the disc is assumed to be homogeneous, isotropic and linearly viscoelastic with complex shear modulus $G(\omega)$, where $\omega = 2\pi f$ is the angular frequency. The shear waves in the disc are associated with the displacement $v(r,t) = u_\phi(r,t)$, the shear strain $\gamma(r,t) = \gamma_{r\phi}(r,t)$, and the shear stress $\tau(r,t) = \tau_{r\phi}(r,t)$, where (r,ϕ,z) are cylindrical coordinates and t is time. These dependent variables are interrelated through $\hat{\tau} = G\hat{\gamma}$ and $\hat{\gamma} = \partial\hat{v}/\partial r - \hat{v}/r$, where the notation $\hat{f}(r,\omega)$ is used for the Fourier transform $\int_{-\infty}^{\infty} f(r,t)e^{-i\omega t}\,dt$ with respect to t of the function $f(r,t)$.

In terms of displacement, the shear waves in the disc are governed by the differential equation

$$r^2\frac{\partial^2\hat{v}}{\partial r^2} + r\frac{\partial\hat{v}}{\partial r} + [(\beta r)^2 - 1]\hat{v} = 0, \tag{1}$$

where $\beta = \omega/c_T$ is a complex wavenumber and $c_T = (G/\rho)^{1/2}$ is a complex wave speed. The general solution of this equation is a linear combination of the Hankel functions $H_1^{(1)}(\xi)$ and $H_1^{(2)}(\xi)$ with $\xi = \beta r$, which have the asymptotic expansions $(2/\pi\xi)^{1/2}e^{-i3\pi/4}e^{i\xi}$ and $(2/\pi\xi)^{1/2}e^{i3\pi/4}e^{-i\xi}$, respectively, for large ξ. By inverse Fourier transformation and from properties of the function $G(\omega)$ (real part even positive function of ω and imaginary part odd function of ω, positive for $\omega > 0$) it can be shown that these asymptotic expressions represent damped shear waves which propagate in the directions of decreasing and increasing r, respectively. Therefore, the general solution of Eq. (1) can be written as

$$\hat{v} = \hat{v}_p H_1^{(2)}(\beta r) + \hat{v}_n H_1^{(1)}(\beta r), \tag{2}$$

where $\hat{v}_p(\omega)$ and $\hat{v}_n(\omega)$ represent the displacement amplitudes of outgoing and ingoing shear waves, respectively.

By Eq. (2) and the differentiation rule $(d/d\xi)H_1^{(i)}(\xi) = H_0^{(i)}(\xi) - (1/\xi)H_1^{(i)}(\xi)$ $(i = 1, 2)$ the general solution for the shear strain $\hat{\gamma} = \partial\hat{v}/\partial r - \hat{v}/r$ in the disc can be expressed as

$$\hat{\gamma} = \hat{\gamma}_p A(\beta r) + \hat{\gamma}_n B(\beta r) \tag{3}$$

with

$$A(\xi) = H_0^{(2)}(\xi) - \frac{2}{\xi}H_1^{(2)}(\xi), \quad B(\xi) = H_0^{(1)}(\xi) - \frac{2}{\xi}H_1^{(1)}(\xi), \tag{4}$$

where $\hat{\gamma}_p = \beta\hat{v}_p$ and $\hat{\gamma}_n = \beta\hat{v}_n$ represent the shear strain amplitudes of outgoing and ingoing shear waves, respectively.

2.2. Boundary conditions and solutions for shear strain

It is assumed that the disc is loaded by a transient shear stress $\hat{\tau}(a,\omega) = \hat{\tau}_a(\omega)$ on its inner boundary. In terms of shear strain, this corresponds to the boundary condition

$$\hat{\gamma}(a,\omega) = \hat{\gamma}_a(\omega) = \frac{\hat{\tau}_a(\omega)}{G(\omega)}. \tag{5}$$

For an *infinite disc* $(b = \infty)$ there are no ingoing shear waves, i.e.,

$$\hat{\gamma}_n = 0. \tag{6}$$

In this case, the general solution (3) and the boundary conditions (5) and (6) give

$$\hat{\gamma} = \frac{A(\beta r)}{A(\beta a)}\hat{\gamma}_a. \tag{7}$$

For a *finite disc* with free outer boundary $\hat{\tau}(b,\omega)=0$ and therefore

$$\hat{\gamma}(b,\omega)=0. \tag{8}$$

In this case, the general solution (3) and the boundary conditions (5) and (8) give

$$\hat{\gamma}=\frac{B(\beta b)A(\beta r)-A(\beta b)B(\beta r)}{B(\beta b)A(\beta a)-A(\beta b)B(\beta a)}\hat{\gamma}_a. \tag{9}$$

2.3. Identification of complex shear modulus

It is now assumed that $\hat{\gamma}(r_1,\omega)=\hat{\gamma}_1^M(\omega)$ and $\hat{\gamma}(r_2,\omega)=\hat{\gamma}_2^M(\omega)$ are obtained from ideal measurements of shear strains at the radii $r=r_1$ and r_2, respectively, with $a<r_1<r_2<b$. Then, by Eq. (7) for the infinite disc and Eq. (9) for the finite disc, there is the relation

$$\hat{\gamma}_1^M\Gamma_2(\beta)-\hat{\gamma}_2^M\Gamma_1(\beta)=0 \tag{10}$$

between these shear strains. The functions $\Gamma_i(\beta)$ $(i=1,\ 2)$ are independent of the excitation $\hat{\gamma}_a(\omega)$ and are taken as

$$\Gamma_i(\beta)=A(\beta r_i) \tag{11}$$

for the infinite disc and

$$\Gamma_i(\beta)=B(\beta b)A(\beta r_i)-A(\beta b)B(\beta r_i) \tag{12}$$

for the finite disc.

For discrete angular frequencies ω_j at which shear waves are generated in the disc, Eq. (10) can generally be solved for $\beta(\omega_j)$. Then, by using the relations $\beta(\omega_j)=\omega_j/c_T(\omega_j)$ and $c_T(\omega_j)=[G(\omega_j)/\rho]^{1/2}$, one can obtain the non-parametric result

$$G(\omega_j)=\rho\left[\frac{\omega_j}{\beta(\omega_j)}\right]^{1/2} \tag{13}$$

for the complex shear modulus. Numerical difficulties may occur at frequencies where the excitation of the disc is weak.

Parametric results for the complex shear modulus can be obtained by using, e.g., the three-parameter viscoelastic standard model

$$G(\omega_j,\mathbf{p})=G^e\frac{G^d+\mathrm{i}\omega_j\eta^d}{G^e+G^d+\mathrm{i}\omega_j\eta^d} \tag{14}$$

with parameter vector $\mathbf{p}=[G^e,G^d,\eta^d]^{\mathrm{T}}$ illustrated in Fig. 1. For this model, the complex wavenumber can be expressed

$$\beta(\omega_j,\mathbf{p})=\omega_j\left[\frac{\rho}{G(\omega_j,\mathbf{p})}\right]^{1/2}. \tag{15}$$

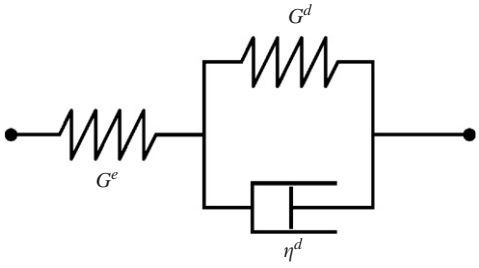

Fig. 1. Three-parameter viscoelastic standard model.

If this expression and measured shear strains $\hat{\gamma}_1^M(\omega_j)$ and $\hat{\gamma}_2^M(\omega_j)$, obtained from a real or simulated experiment, are substituted into the left member of Eq. (10) for a given parameter vector $\mathbf{p}$, the result will be

$$\hat{\gamma}_1^M(\omega_j)\Gamma_2[\beta(\omega_j,\mathbf{p})] - \hat{\gamma}_2^M(\omega_j)\Gamma_1[\beta(\omega_j,\mathbf{p})] = e_j(\mathbf{p}), \tag{16}$$

where the residual $e_j(\mathbf{p})$ at angular frequency ω_j is generally different from zero. A global measure of the deviation between experimental data, represented by $\hat{\gamma}_1^M(\omega_j)$ and $\hat{\gamma}_2^M(\omega_j)$, and model prediction, represented by $\Gamma_1[\beta(\omega_j,\mathbf{p})]$ and $\Gamma_2[\beta(\omega_j,\mathbf{p})]$, at the angular frequencies $\omega_1, \omega_2, \ldots, \omega_n$ is given by

$$\|\mathbf{e}(\mathbf{p})\|^2 = \overline{\mathbf{e}(\mathbf{p})}^{\mathrm{T}}\mathbf{e}(\mathbf{p}) = |e_1(\mathbf{p})|^2 + |e_2(\mathbf{p})|^2 + \cdots + |e_n(\mathbf{p})|^2, \tag{17}$$

where $\mathbf{e}(\mathbf{p}) = [e_1(\mathbf{p}), e_2(\mathbf{p}), \ldots, e_n(\boldsymbol{p})]^{\mathrm{T}}$ is the residual vector. The parameter vector $\mathbf{p}$ of the material model is determined as the one that minimizes this expression.

The error $e_j = e(\omega_j)$ at the angular frequency ω_j for the optimal parameter vector $\mathbf{p} = \mathbf{p}_{\mathrm{opt}}$ is defined as the ratio of the magnitude of the residual $e_j(\mathbf{p}_{\mathrm{opt}})$ to that of the first term of Eq. (16), i.e.,

$$e_j^* = \frac{|e_j(\mathbf{p}_{\mathrm{opt}})|}{|\phi_j(\mathbf{p}_{\mathrm{opt}})|}, \quad \phi_j(\mathbf{p}_{\mathrm{opt}}) = \hat{\gamma}_1^M(\omega_j)\Gamma_2[\beta(\omega_j,\mathbf{p}_{\mathrm{opt}})]. \tag{18}$$

If the conditions are such that the complete strain history of the outgoing shear wave generated at the inner radius $r = a$ can be measured at the radii $r = r_1$ and r_2 before a reflected shear wave from the outer radius $r = b$ has reached $r = r_2$, the disc can be considered infinite. Computationally, this case is much easier than that of a finite disc where the measured shear strains consist of superimposed contributions from out- and ingoing shear waves. In the non-parametric and parametric identifications that follow in Sections 3 and 4; therefore, the conditions will be considered to be such that the disc can be taken as infinite. Consequently, all identification procedures in these sections will make use of Eq. (11), valid for an *infinite* disc. In contrast, the numerical simulations of experimental tests in Section 3 will make use of Eq. (9), valid for a *finite* disc.

3. Identification based on numerical simulations

In order to study the identification procedures of Section 2.3, identification of the complex shear modulus of a linearly viscoelastic material was first based on numerical simulations of experimental tests. The material of the disc was described by the three-parameter viscoelastic standard model with $G^e = 1.005\,\mathrm{GPa}$, $G^d = 1.837\,\mathrm{GPa}$ and $\eta^d = 0.122\,\mathrm{MPa\,s}$, and the density was taken to be $\rho = 915\,\mathrm{kg/m^3}$. The constitutive parameters were based on non-parametric data for polypropylene (PP) obtained in experimental tests with a bar specimen [12]. The radii of the disc were taken as those of the hub and the rim, $a = 30\,\mathrm{mm}$ and $b = 500\,\mathrm{mm}$, of the disc used in the experimental tests to be described in Section 4. Two cases of load were considered. In both of them, the shear stress $\tau_a(t)$ on the inner radius of the disc was prescribed as a rectangular pulse. In the first case, the duration t_0 of the load was taken as 240 μs. In the second case, it was taken five times shorter, i.e., 48 μs.

The simulated shear strains $\gamma_1^M(t)$ and $\gamma_2^M(t)$ were obtained from Eq. (9) for a finite disc. They were regarded as measured at the radii $r_1 = 60$ and $r_2 = 96\,\mathrm{mm}$, respectively, and included the effects of both outgoing and ingoing shear waves, similarly as in the experimental tests of Section 4. From them, the complex shear modulus $G(\omega)$ was identified non-parametrically by use of Eqs. (10), (11) and (13), and parametrically by use of Eqs. (11) and (14)–(17). Thus, in both identification procedures the effects of ingoing waves, if any, were neglected. Transformations between the time and frequency domains were carried out by use of the fast Fourier transform algorithm with a sampling frequency of 1 MHz. The minimization of the expression given by Eq. (17) was carried out with the function *fminsearch* of MATLAB Version 7.2. This function is a local minimizer, which uses a Nelder–Meade simplex search. The constitutive parameters used in the simulated tests, and the start values and results of parametric identification are summarized in Table 1. It was verified that the result for the complex shear modulus did not depend significantly on these start values.

The first simulated identification test is illustrated in Fig. 2, where (a) shows the prescribed load on the disc and (b) the measured shear strains. The arrival at radius r_2 of the shear wave reflected from the rim of the disc is indicated by R. Only the measured shear strains between the two full vertical lines were used. In this

Table 1
Standard linear solid parameters in numerical simulations

Parameter	Simulation value	Start value	Estimated value	
			Test 1	Test 2
G^e (GPa)	1.005	1.623	0.9613	1.004
G^d (GPa)	1.837	0.952	0.7133	1.827
η^d (MPa s)	0.122	0.064	0.1682	0.123

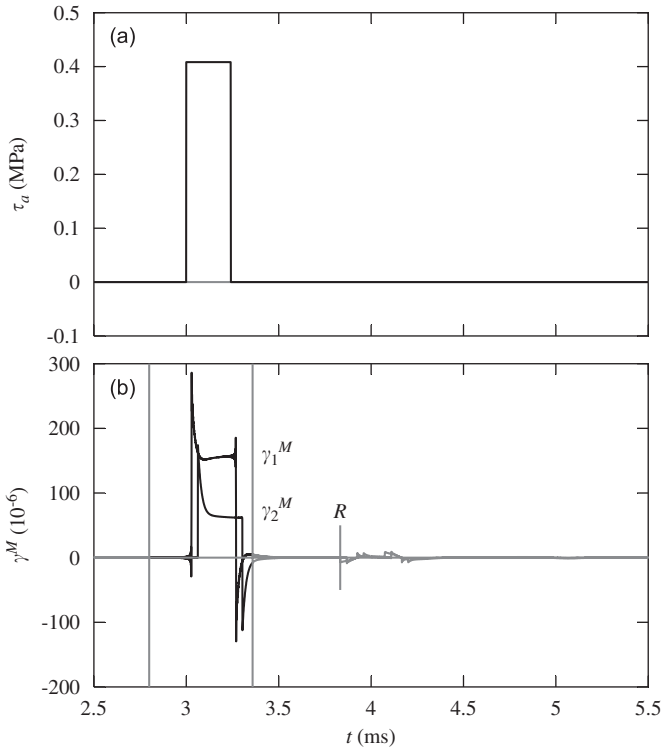

Fig. 2. (a) Rectangular shear stress pulse excitation τ_a and (b) measured shear strains γ_1^M and γ_2^M versus time t in 1st simulated identification test. The identification was based on the measured shear strains between the two full vertical lines, and R indicates the arrival at radius r_2 of the shear wave reflected from the rim of the disc.

way, the ingoing shear wave reflected from the rim was excluded in accord with the employment of the infinite-disc model for identification. Also, the tail of the outgoing shear wave was slightly truncated. This truncation was not necessary; it was made in order to illustrate the errors it generates.

Results for the complex shear modulus G up to 20 kHz are shown in Fig. 3, where the upper curves in each diagram are the real parts and the lower curves are the imaginary parts. Fig. 3(a) shows the result of non-parametric identification (thin curves with dot marks), and Fig. 3(b) shows that of parametric identification (thick curves) carried out in the frequency range 1–20 kHz. In both diagrams, the results of identification are compared with the parametric model used in the simulation (thin curves).

The second simulated identification test is illustrated in Fig. 4. Also here it can be seen that outgoing shear waves only were used in accord with the employment of the infinite-disc model for identification. In this case, however, there was practically no truncation due to the short duration of the load. Results for the complex shear modulus G, with explanations as above, are shown in Fig. 5, where (a) shows the result of

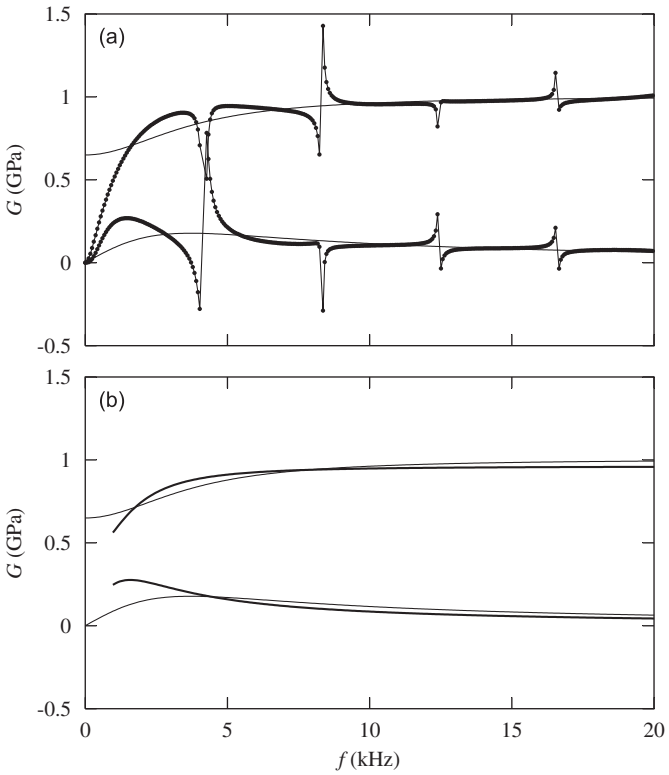

Fig. 3. Complex shear modulus G versus frequency f used in simulation (thin curves) and obtained from 1st simulated identification test. Upper curves in each diagram show real parts and lower curves imaginary parts: (a) non-parametric (thin curves with dot marks) and (b) parametric (thick curves) results.

non-parametric identification, and (b) shows that of parametric identification carried out in the frequency range 1–20 kHz. In both diagrams, the results of identification are compared with the parametric model used in the simulation (thin curves).

4. Identification based on experimental tests

Experimental identification tests were carried out with the set-up shown in Fig. 6. A disc made of PP with 6 mm thickness and outer diameter 1000 mm was attached to a hub at its centre. The hub, designed for axial symmetry, sufficient strength and low inertia, is shown in Fig. 7(a). It consisted of a 2.7 mm thick circular steel plate with diameter 60 mm and a 3.6 mm thick aluminium ring with diameters 17 and 60 mm. The plates with the disc in between were kept together by 16 M4 screws, half of them evenly distributed along a circle with radius 30 mm and half at intermediate positions along a circle with radius 50 mm. The steel plate was welded to one end of a cylindrical steel shaft with length 6470 mm and diameter 20 mm. At its opposite end, the shaft was preloaded in torsion between two clamps shown in Fig. 7(b). When the clamp closest to the disc was suddenly released by fracturing a pre-notched bolt, a torsional wave was generated in the shaft. This wave, with length approximately twice the inter-clamp distance, propagated towards the disc at which it was partially reflected. As a result, the disc was loaded by a transient torque producing an outgoing shear wave. The length of the shaft was chosen so that torsional waves, after reflections at the two ends of the shaft, would not disturb shear strain measurements on the disc.

The strain gauges used to measure shear strains on the disc were double-element gauges with active length 2 mm (MTL, QFCT-2-350-11-6F-1LT). At each radial position, two strain gauges were mounted opposite to each other on each side of the disc so that their elements were oriented in directions $\pm 45^\circ$ relative to the radial

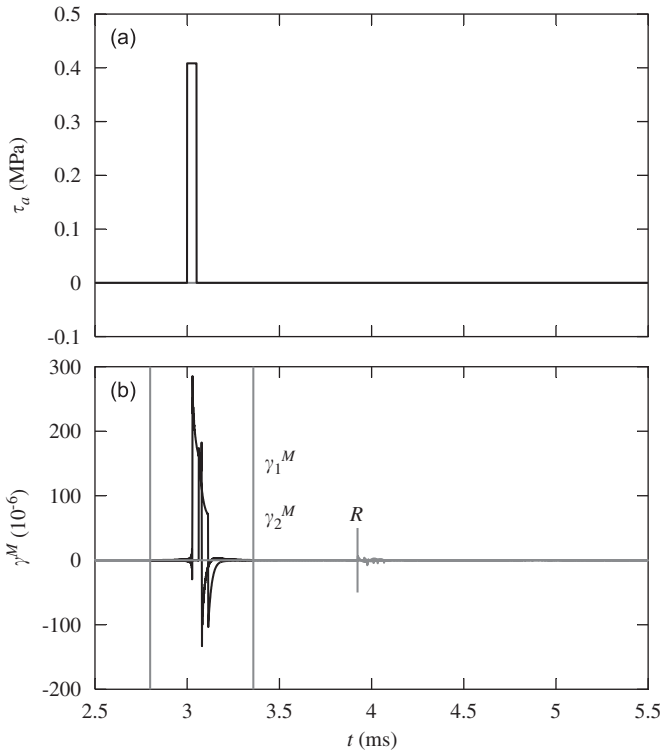

Fig. 4. (a) Rectangular shear stress pulse excitation τ_a and (b) measured shear strains γ_1^M and γ_2^M versus time t in 2nd simulated identification test. The identification was based on the measured shear strains between the two full vertical lines, and R indicates the arrival at radius r_2 of the shear wave reflected from the rim of the disc.

direction. The four elements of such a strain gauge pair at each radial position formed branches of a Wheatstone bridge so that the output voltage of the bridge was proportional to the shear strain but insensitive to bending. The output signals from the bridges constituted input to bridge amplifiers (Measurement Group, 2210), the output signals of which were sampled simultaneously at 1 MHz and recorded by use of a 12-bit data acquisition board (Strategic Test, UF-3122). Shunt calibration was used.

Three experimental tests were carried out at room temperature of approximately 22 °C. The amplitude of the load was controlled by the preload of the shaft (high, low), and the duration of the load by the distance between the clamps (long distance 165 mm, and short distance 110 mm). In Tests a–c, the preload of the shaft and the distance between the clamps were taken as high-long, low-long and low-short, respectively. The same non-parametric and parametric identification procedures, based on an infinite disc, were used as for the simulated tests. Also, the parametric identification was carried out in the same frequency interval 3–20 kHz and made use of the same parameter start values as for these tests. The parameter start values and results of parametric identification are summarized in Table 2. It was verified that the result for the complex shear modulus did not depend significantly on these start values.

The results of the experimental identification tests are shown in Figs. 8–10. Figs. 8(a)–(c) show the measured shear strains γ_1^M and γ_2^M from Tests a–c, respectively. The identifications were based on the measured shear strains between the two full vertical lines. In this way, similarly as in the simulated tests, the reflected shear wave from the rim of the disc was excluded in accord with the employment of the infinite-disc model for identification. Non-parametric and parametric results up to 20 kHz for the complex shear modulus G from Tests a–c are shown in Figs. 9(a)–(c), respectively, where the upper curves in each diagram are the real parts and the lower curves are the imaginary parts. The parametric identification was carried out in the frequency range 3–20 kHz. The parametric results can be compared in Fig. 10(a), and the corresponding results for the error $e^*(\omega_j) = e_j^*$, defined in Eq. (18), are shown in Fig. 10(b).

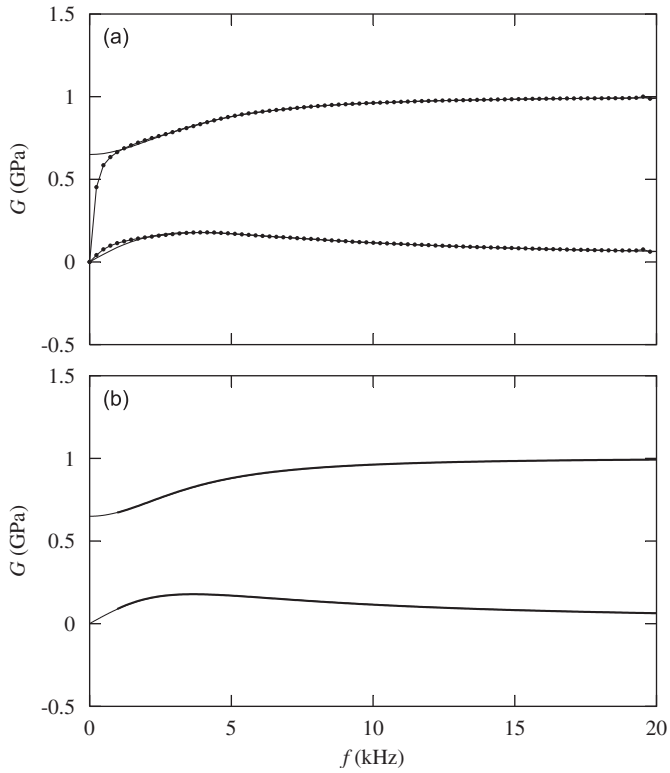

Fig. 5. Complex shear modulus G versus frequency f used in simulation (thin curves) and obtained from 2nd simulated identification test. Upper curves in each diagram show real parts and lower curves imaginary parts: (a) non-parametric (thin curves with dot marks) and (b) parametric (thick curves) results.

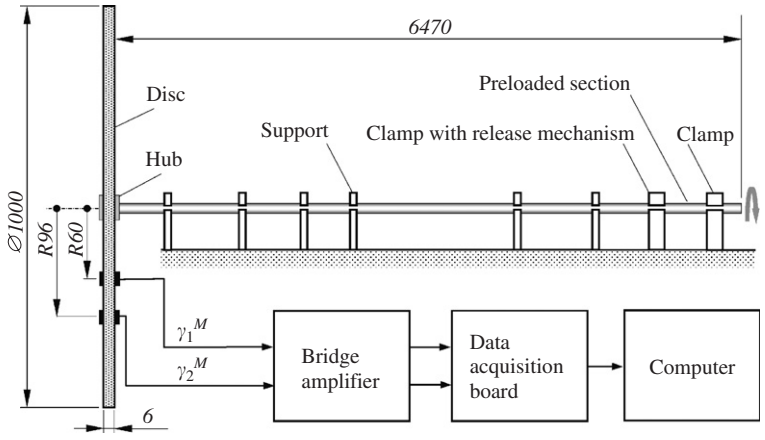

Fig. 6. Experimental set-up.

5. Discussion

A method for identification of complex shear modulus from measured shear strains on a circular disc subjected to a transient torque at its centre has been established. The method is based on the evolution of an outgoing shear wave between two radial positions at which the associated shear strains are measured. Therefore, the disc must have a certain minimum size so that the front of the outgoing shear wave is able to

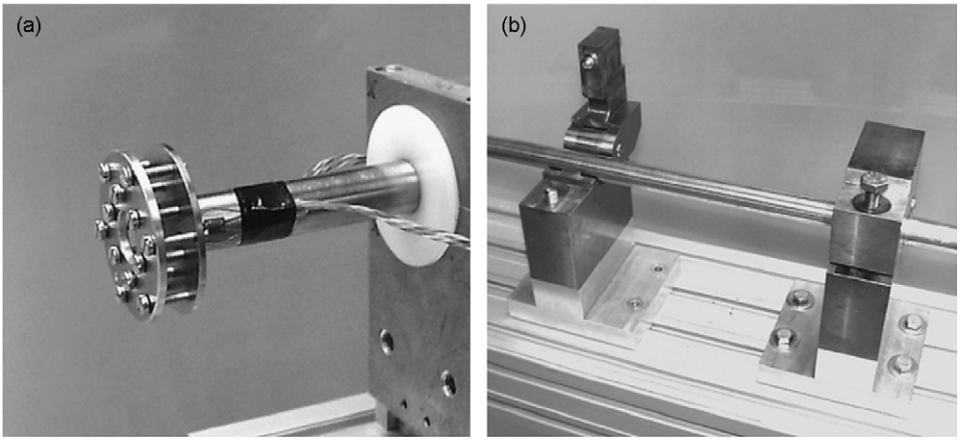

Fig. 7. Details of experimental set-up: (a) hub of the disc and (b) clamps and release mechanism.

Table 2
Standard linear solid parameters in experimental tests

Parameter	Start value	Estimated value		
		Test a	Test b	Test c
G^e (GPa)	1.623	1.231	1.186	1.170
G^d (GPa)	0.952	3.703	3.636	3.329
η^d (MPa s)	0.064	0.116	0.128	0.183

travel from the outermost strain gauge position to the rim of the disc and back without interfering with the outgoing shear wave at this position during the period of measurement. Clearly, this minimum size is related to the duration of the load. The method is a two-dimensional analogue of methods based on the evolution of a wave between two axial positions of a bar specimen, e.g., Refs. [15–17].

It has also been shown that, by considering the boundary condition at the rim of the disc, one can identify the complex shear modulus without being restricted to outgoing shear waves. This procedure is a two-dimensional analogue of another procedure used for bar specimens, e.g., Refs. [5,7,10–12], and has the advantage of not requiring a minimum size of the disc specimen. However, it is computationally complex and may lead to reduced accuracy.

The two-dimensional shear wave solutions used are exact in the sense of three-dimensional theory and therefore, in principle, there is no frequency beyond which the theoretical basis of the methods is not valid. However, there are practical limitations as shear waves must be generated in accord with the boundary condition (5), stating that there must be no variation of shear stress in the circumferential direction or through the thickness of the disc.

In Fig. 3(a), which shows the non-parametric result from the first simulated identification test, it can be seen that the identification is inaccurate at the frequency zero and at certain non-zero frequencies. The inaccuracy at $f = 0$ is due to the truncation of the measured shear strains which can be seen in Fig. 2(b). The truncation leads to errors in the Fourier transforms $\hat{\gamma}_i^M(0) = \int_{-\infty}^{\infty} \gamma_i^M(t)\,\mathrm{d}t$ of the measured shear strains and therefore, no matter how small these errors are, Eq. (10) generally has a non-zero solution for the wavenumber $\beta(0)$. With this erroneous result, Eq. (13) gives $G(0) = 0$ for the complex shear modulus, which is incorrect for the real part. The non-zero frequencies are those at which the Fourier transform of the rectangular loading pulse $\tau_a(t)$ with duration $t_0 = 240\,\mu\mathrm{s}$ (Fig. 2(a)) is zero, i.e., $f = n/t_0$ ($n = 1, 2, 3, \ldots$) or 4.17, 8.34, 12.5, 16.7, … kHz. At these problematic frequencies, there is no excitation of the disc, and this leads to large errors. In the first simulated identification test, where four non-zero problematic frequencies are present in the frequency range

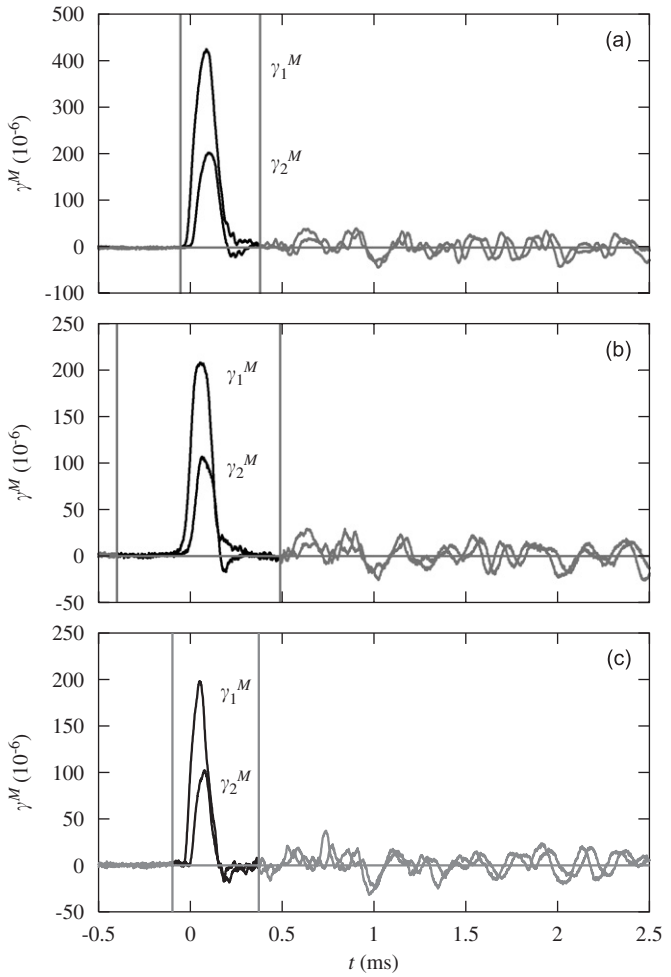

Fig. 8. Measured shear strains γ_1^M and γ_1^M versus time t in experimental identification tests employing load with (a) high amplitude and long duration, (b) low amplitude and long duration, and (c) low amplitude and short duration. The identification was based on the measured shear strains between the two vertical lines.

of interest, 0–20 kHz, the parametric results shown in Fig. 3(b) are more accurate and representative of the material behaviour than the non-parametric ones.

The disturbing inaccuracies of Fig. 3(a) are considerably reduced in Fig. 5(a), which shows the non-parametric result of the second simulated identification test. Here the duration of the loading pulse (Fig. 4(a)) is smaller by a factor of five, while the time interval used for the measured shear strains (2.80, 3.36) ms, is the same as in the first simulated identification test. As a consequence, the effect of truncation is reduced and therefore the result for the complex shear modulus is much more accurate near $f = 0$. Furthermore, the problematic frequencies 20.8, 41.7, 62.5, … kHz are five times higher, and therefore they have moved outside the frequency range of interest, 0–20 kHz. Therefore, the non-parametric (Fig. 5(a)) and parametric (Fig. 5(b)) results obtained from the second identification test are significantly more accurate than those obtained from the first. Another way of improving the accuracy would be to exclude measurement data at and around the problematic frequencies.

Figs. 8(a)–(c) show that the tails of the measured shear strains in the experimental identification tests fade out within the time intervals on which the identification was based, similarly as in the second simulated identification test (Fig. 4(b)). Later, and quite abruptly, the shear strains become oscillatory. This appears to be mainly due to waves that are multiply reflected between the rim and the hub of the disc. Sign reversals of the shear strains occur at the rim, which is free.

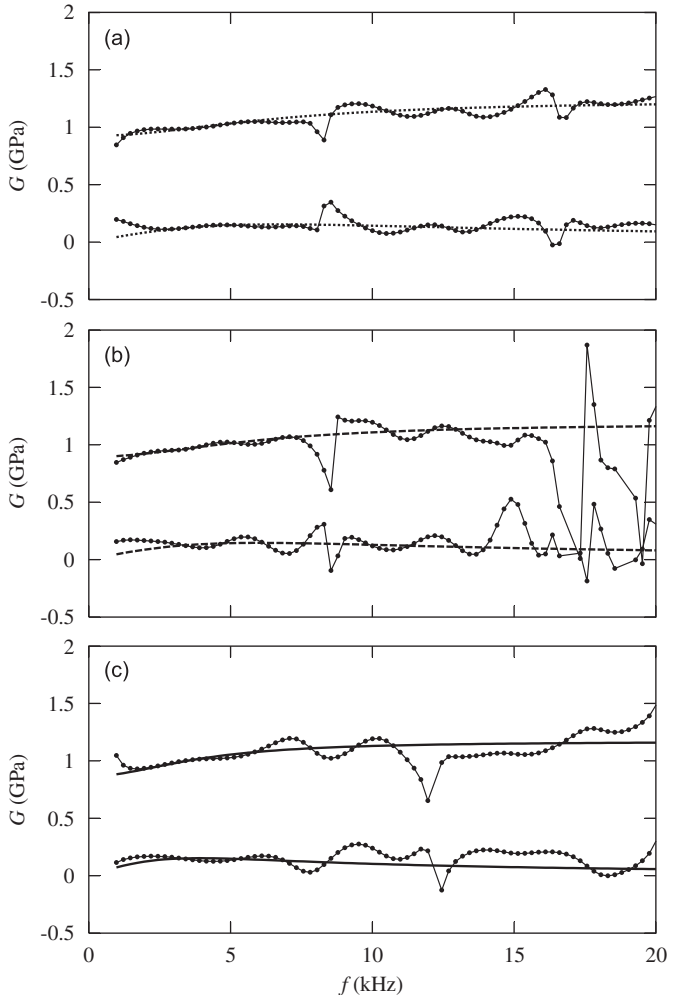

Fig. 9. Complex shear modulus G versus frequency f from experimental identification tests employing load with (a) high amplitude and long duration, (b) low amplitude and long duration and (c) low amplitude and short duration. Upper curves in each diagram show real parts and lower curves imaginary parts: Non-parametric (thin curves with dot marks) and parametric (thick curves) results.

In Figs. 9(a)–(c), which show the non-parametric and parametric results for the complex shear modulus from the experimental identification Tests a–c, respectively, irregularities can be observed near the frequency zero and at certain non-zero frequencies. This behaviour is similar to that in the first simulated test. In Figs. 9(a) and (b), with the same approximate duration of the loading pulse, the lowest frequency with irregular result is approximately 8.3 kHz. In Fig. 9(c), with a shorter loading pulse, the first problematic frequency is higher, approximately 11.9 kHz. In the three cases, the parametric results appear to be more representative than the non-parametric ones, similarly as in the simulations.

Fig. 10(a) shows that there is good agreement between the parametric results for the complex shear modulus of PP in the three experimental identification tests, although, as shown by Fig. 10(b), large errors e appear at the problematic frequencies. In particular, the agreement between the parametric results obtained in experimental Tests a and b are in accord with the assumed linearity of the disc material. In these tests, the measured shear strain pulses had similar durations but amplitudes, which differed by a factor of two (approximately 400×10^{-6} and 200×10^{-6}, respectively). Compared with the parametric results of Fig. 10(a) for PP, obtained with a disc specimen, the non-parametric results of Ref. [12] for the same material, obtained with a bar specimen, have somewhat lower real part and somewhat higher imaginary part. Because of different

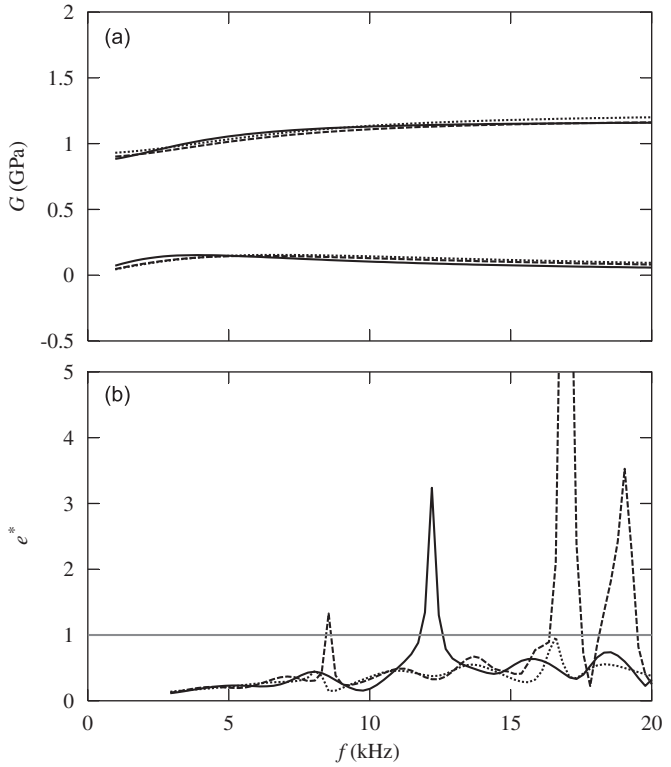

Fig. 10. Upper curves in (a) show parametric complex shear modulus G and (b) error e versus frequency f from experimental identification tests employing load with high amplitude and long duration (dotted curves), low amplitude and long duration (dashed curves) and low amplitude and short duration (solid curves). Upper curves in each diagram show real parts and lower curves imaginary parts.

manufacturers, manufacturing processes, batches, testing conditions, etc., the discrepancies observed, of the order of 15%, are not unexpected.

It follows from the results that it is desirable to generate narrow shear strain pulses in the disc specimens. These pulses must be axially symmetric and have sufficient amplitude. One advantage with reduced pulse width, for a given disc size, is reduced inaccuracy at low frequencies due truncation of the measured shear strains. Another is that the problematic frequencies increase and may move outside the frequency range of interest. The generation of narrow axially symmetric pulses with sufficient amplitude requires practical considerations, which in this study led to the use of a preloaded shaft, a hub with low inertia (Fig. 7(a)) and a fast release mechanism (Fig. 7(b)). Other possible solutions may be based on the use of rotational impact, as in Ref. [12], or piezoelectric actuation.

6. Conclusions

The main conclusions of this study can be summarized as follows: (i) The complex shear modulus of an isotropic and linearly viscoelastic material can be identified on the basis of the evolution of an outgoing shear wave between two radial positions on a disc at which the associated shear strains are measured. (ii) The two-dimensional shear wave solutions used are exact in the sense of three-dimensional theory, and therefore there is, in principle, no frequency beyond which the theoretical basis is not valid. (iii) The method requires a minimum disc size related to the duration of the load. (iv) The non-parametric results become inaccurate at frequencies near zero and where the excitation of the disc is weak or non-existent. (v) These frequencies may be removed from the frequency range of interest by sufficiently decreasing the duration of the loading pulse. Alternatively, the required size of the disc can be reduced. (vi) If there are problematic frequencies within the range of interest, the results of parametric identification are more accurate and representative than those of

non-parametric identification. (vii) Parametric results from experimental tests with loads having different amplitudes and durations agree well with each other in accord with the assumed linearity of the tested PP material. (viii) The complex shear modulus of an isotropic and linearly viscoelastic material can be identified similarly also without restriction to outgoing shear waves. This procedure has the advantage of not requiring a minimum size of the disc but is computationally complex and may lead to reduced accuracy.

Acknowledgements

Funding from the Swedish Research Council (contract 2004-5169) is gratefully acknowledged. The authors also thank Mr. Åke Dahlberg for accurately making the critical pieces of equipment.

References

[1] W. Flügge, *Viscoelasticity*, Springer, Berlin, Heidelberg, 1975.
[2] P.S. Theocaris, Interrelation between dynamic moduli and compliances in polymers, *Kolloid-Zeitschrift und Zeitschrift für Polymere* 235 (1960) 1182–1188.
[3] T. Pritz, Frequency dependences of complex moduli and complex Poisson's ratio of real solid materials, *Journal of Sound and Vibration* 214 (1998) 83–104.
[4] J.L. Buchanan, Numerical solution for the dynamic moduli of a viscoelastic bar, *Journal of the Acoustical Society of America* 81 (1987) 1775–1786.
[5] B. Lundberg, R.H. Blanc, Determination of mechanical material properties from the two-point response of an impacted linearly viscoelastic rod specimen, *Journal of Sound and Vibration* 126 (1988) 97–108.
[6] S. Ödeen, B. Lundberg, Determination of complex modulus from measured end-point accelerations of an impacted rod specimen, *Journal of Sound and Vibration* 165 (1993) 1–8.
[7] B. Lundberg, S. Ödeen, In situ determination of the complex modulus from strain measurements on an impacted structure, *Journal of Sound and Vibration* 167 (1993) 413–419.
[8] A.J. Hull, An inverse method to measure the axial modulus of composite materials under tension, *Journal of Sound and Vibration* 195 (1996) 545–551.
[9] M. Soula, T. Vinh, Y. Chevalier, T. Beda, C. Esteoule, Measurements of isothermal complex moduli of viscoelastic materials over a large range of frequencies, *Journal of Sound and Vibration* 205 (1997) 167–184.
[10] L. Hillström, M. Mossberg, B. Lundberg, Identification of complex modulus from measured strains on an axially impacted bar using least squares, *Journal of Sound and Vibration* 230 (2000) 689–707.
[11] M. Mossberg, L. Hillström, L. Abrahamsson, Parametric identification of viscoelastic materials from time and frequency domain data, *Inverse Problems in Engineering* 9 (2001) 645–670.
[12] S. Mousavi, D.F. Nicolas, B. Lundberg, Identification of complex moduli and Poisson's ratio from measured strains on an impacted bar, *Journal of Sound and Vibration* 277 (2004) 971–986.
[13] H. Kolsky, S.S. Lee, The propagation and reflection of stress pulses in linear viscoelastic media, Brown University Technical Report No. 5, 1962.
[14] P.S. Theocaris, N. Papadopoulou, Propagation of stress waves in viscoelastic media, *Polymer* 19 (1978) 215–219.
[15] R.H. Blanc, *Détermination de l'Équation de Comportement des Corps Viscoélastiques Linéaires par une Méthode d'Impulsion*, PhD Thesis, Université d'Aix-Marseille, 1971. (Published in part in Problèmes de la rhéologie (W.K. Nowacki, editor) 65–85, IPPT PAN, Warsaw 1973.)
[16] R.H. Blanc, Progress in pulse testing methods for viscoelastic solids, *Proceedings of the Second National Congress on Theoretical and Applied Mechanics*, Varna, Bulgarian Academy of Science Publication, Sofia, Vol. 2, 1976, pp. 555–564.
[17] R.H. Blanc, Transient wave propagation methods for determining the viscoelastic properties of solids, *Journal of Applied Mechanics* 60 (1993) 763–768.
[18] Y. Sogabe, K. Kishida, K. Nakagawa, Wave propagation analysis for determining the dynamic properties of high damping alloys, *Bulletin of the Japan Society of Mechanical Engineers* 25 (1982) 321–327.
[19] Y. Sogabe, M. Tsuzuki, Identification of the dynamic properties of linear viscoelastic materials by the wave propagation testing, *Bulletin of the Japan Society of Mechanical Engineers* 29 (1986) 2410–2417.
[20] L. Hillström, U. Valdek, B. Lundberg, Estimation of the state vector and identification of the complex modulus of a beam, *Journal of Sound and Vibration* 261 (2003) 653–673.